A hypoplastic model for mechanical response of unsaturated soils

David Mašín

(corresponding author)
Charles University
Faculty of Science
Institute of Hydrogeology, Engineering Geology and Applied Geophysics
Albertov 6
12843 Prague 2, Czech Republic
E-mail: masin@natur.cuni.cz
Tel: +420-2-2195 1552, Fax: +420-2-2195 1556

Nasser Khalili

The University of New South Wales
School of Civil and Environmental Engineering
Sydney NSW 2052, Australia
E-mail: n.khalili@unsw.edu.au

March 12, 2008

Submitted to *International Journal for Numerical and Analytical Methods in Geomechanics*

Keywords

unsaturated soils, hypoplasticity, effective stress, non-linearity, collapse

Abstract

A new constitutive model is developed for the mechanical behaviour of unsaturated soils based on the theory of hypoplasticity and the effective stress principle. The governing constitutive relations are presented and their application is demonstrated using several experimental data from the literature. Attention is given to the stiffening effect of suction on the mechanical response of unsaturated soils and the phenomenon of wetting-induced collapse. All model parameters have direct physical interpretation, procedures for their quantification from test data are highlighted. Quantitative predictions of the model are presented for wetting, drying and constant suction tests.

1 Introduction

The twenty years of research on hypoplasticity, a particular class of incrementally non-linear constitutive models, have led to a significant progress in the theoretical basis and applications of this alternative approach to constitutive modelling of geomaterials. The predictive capabilities of hypoplastic models compete with those of advanced models from other constitutive frameworks [35, 47, 17, 32], yet they require only limited number of material parameters. This, together with the availability of robust algorithms for their implementation into numerical codes [11], makes hypoplasticity a promising approach for use in practical applications.

The theoretical basis for this class of constitutive models has been put forward independently by researchers in Karlsruhe (see, e.g., [25]) and Grenoble [8]. The early models of the Karlsruhe school were developed by trial-and-error [24] and had only limited capabilities. In contrast, the more recent and evolved hypoplastic models cover a wide range of geomaterials, namely granular materials [49], soils with a low friction angle [18] and clays [30]. Procedures to incorporate anisotropy [39, 52, 53], viscosity [37, 16], structure [33, 31] and the elastic behaviour in the very small strain range and the effects of recent history [40] are currently available. To date, however, most contributions on the constitutive modelling of soils using the theory of hypoplasticity have been in the domain of saturated soils. Extension of this class of constitutive models to unsaturated soils is thus still an open field for research.

Many of the current constitutive models for the behaviour of unsaturated soils are almost exclusively based on the conventional elastoplastic framework. Notable examples include contributions of Alonso et al. [1], Kogho et al. [23], Modaressi and Abou-Bekr [36], Wheeler and Sivakumar [50], Loret and Khalili [27, 28], Vaunat et al. [48], Khalili and Loret [22], Gallipoli et al. [13], Wheeler et al. [51], Sheng et al. [44], Borja [6], Ehlers et al. [10] and Santagiuliana and Schrefler [43] among others. Only limited attempts have

been made to incorporate the behaviour of unsaturated soils into non-linear constitutive models (Russell and Khalili [42]; Bolzon et al. [5]).

The first attempt to model unsaturated soil behaviour using the theory of hypoplasticity was put forward by Gudehus [14]. He utilised the effective stress concept (see Sec. 3) with a modified formulation for the scalar factor χ of the basic equation by Bishop [4]. The model predicted, under certain conditions, the behaviour of unsaturated soils subject to suction changes. However, it could not predict compressive volumetric strains that occur in unsaturated soils with an open structure along wetting paths (wetting-induced collapse). Also, it assumed the same limit void ratios for saturated and unsaturated materials, and could not simulate stiffening of the soil structure due to suction increase. This latter shortcoming was later overcome by Bauer et al. [2, 3]. Their model assumed dependence of the limit void ratios of weathered broken rock on the moisture content and thus was able to predict different mechanical responses for different suctions. However, the stress state variable adopted did not include suction, rendering the model incapable of predicting the soil response along wetting and drying paths.

The aim of this paper is to present a more complete treatment of the theory of hypoplasticity for unsaturated soils. The governing constitutive equations are formulated using the notion of critical state and the effective stress principle. Particular attention is given to the stiffening effect of suction on the mechanical response of unsaturated soils and the phenomenon of wetting-induced collapse. A novel approach is proposed for incorporating the suction effects into the hypoplastic models. The new model has basic properties of hypoplastic models, it therefore predicts pre- and post-peak non-linear deformation behaviour of unsaturated soils, and the variation of the soil stiffness with loading direction - important aspects absent from many of the current constitutive models proposed for the behaviour of unsaturated soils. Hydraulic hysteresis is ignored throughout to retain simplicity of the theoretical developments. Smooth transition from saturated to unsaturated states is ensured using the effective stress principle for unsaturated soils. The characteristic features of the model are validated using experimental data from the literature.

The paper is organized as follows. Section 2 is devoted to the presentation of the reference hypoplasticity model for saturated soils. Section 3 epitomizes the role of the effective stress in the behaviour of unsaturated soils and Section 4 is devoted to the development of the proposed hypoplasticity model for unsaturated soils, and how the suction effects are incorporated into the formulation. The calibration of the model is presented in Section 5 and its application to laboratory test data is demonstrated in Section 6. A complex of loading paths including wetting, drying, and constant-suction isotropic consolidation and triaxial compression and extension is considered.

Notations and Conventions: Compact or index tensorial notation is used throughout. Second-order tensors are denoted with bold letters (e.g. $\mathbf{T}$, $\mathbf{N}$) and fourth-order tensors with calligraphic bold letters (e.g. $\boldsymbol{\mathcal{L}}$, $\boldsymbol{\mathcal{A}}$). Symbols "$\cdot$" and ":" between tensors of various orders denote inner product with single and double contraction, respectively. The dyadic product of two tensors is indicated by "$\otimes$", $\|\mathbf{D}\|$ represents the Euclidean norm of $\mathbf{D}$ and the arrow operator is defined as $\vec{\mathbf{D}} = \mathbf{D}/\|\mathbf{D}\|$. The trace operator is defined as ($\mathrm{tr}\,\mathbf{D} = \mathbf{1} : \mathbf{D}$), $\mathbf{1}$ and $\boldsymbol{\mathcal{I}}$ denote second-order and fourth-order unity tensors, respectively. Following

the sign convention of continuum mechanics compression is taken as negative. However, Roscoe's variables $p = -\operatorname{tr}\mathbf{T}/3$ and $\epsilon_v = -\operatorname{tr}\boldsymbol{\epsilon}$, and suction $s = -(u_a - u_w)$, are defined in such a way that they are positive in compression. The operator $\langle x \rangle$ denotes positive part of any scalar function x.

2 Reference model for saturated soils

The reference model for the present derivations, proposed by Mašín [30], is based on the Karlsruhe approach to hypoplasticity [49, 38, 18]. Within this context, the stress-strain rate relationship is written as [15]

$$\mathring{\mathbf{T}} = f_s \left(\boldsymbol{\mathcal{L}} : \mathbf{D} + f_d \mathbf{N} \|\mathbf{D}\| \right) \tag{1}$$

where $\mathring{\mathbf{T}}$ denotes the objective (Zaremba-Jaumann, see [26]) stress rate, $\mathbf{D}$ is the Euler's stretching tensor, $\boldsymbol{\mathcal{L}}$ and $\mathbf{N}$ are fourth- and second-order constitutive tensors and f_s and f_d are two scalar factors, denoted as *barotropy* and *pyknotropy* factors respectively.

The model is conceptually based on the critical state soil mechanics and its five parameters (φ_c, N, λ^*, κ^*, r) have similar physical interpretation as parameters of the Modified Cam clay model [41]. Parameters N and λ^* define the position and the slope of the isotropic normal compression line, following the formulation by Butterfield [7]

$$\ln(1+e) = N - \lambda^* \ln \frac{p}{p_r} \tag{2}$$

where p_r is an arbitrary reference stress, which is considered equal to 1 kPa throughout this paper. The parameters N and λ^* also control the position of the critical state line, with the assumed formulation

$$\ln(1+e) = N - \lambda^* \ln 2 - \lambda^* \ln \frac{p}{p_r} \tag{3}$$

The next parameter, κ^*, controls the slope of the isotropic unloading line and the parameter r the shear stiffness. Finally, φ_c is the critical state friction angle. It controls the size of the critical state locus in the stress space, defined by the formluation according to Matsuoka and Nakai [29]. The model consideres void ratio e as a state variable.

The model requires a limited number of material parameters, nevertheless it predicts complex non-linear behaviour of soils [30], including the variation of stiffness with loading direction [35] and the influence of relative density (overconsolidation ratio) on the soil stiffness, volumetric behaviour and peak friction angle [17].

It is instructive to note that the mathematical formulation of hypoplastic models does not include explicitly state boundary surface (SBS), defined as the boundary of all possible states of a soil element in the *effective stress vs. void ratio space*, as well as it does not include the bounding surface (BS), which is defined in the *effective stress space* as a constant-void-ratio cross-section through the SBS. However, Mašín and Herle [34] demonstrated that implicit in the formulation of the model in [30] is the existence of a SBS whose

form and size can be analytically expressed. This fact is crucial, and will be fully exploited in the sections that follow in extending the reference hypoplastic model for saturated soils to include unsaturation.

3 Effective stress concept for unsaturated soils

Central to the framework presented here is the concept of effective stress which can be defined in the following general form, subject to the solid grains incompressibility constraint [4, 21, 27]

$$\mathbf{T} = \mathbf{T}^{net} - \mathbf{1}\chi s \tag{4}$$

Stress variables without any superscript ($\mathbf{T}$) denote the effective stress, $\mathbf{T}^{net}$ is the net stress defined as $\mathbf{T}^{net} = \mathbf{T}^{tot} - \mathbf{1}u_a$ and $s = -(u_a - u_w)$ is the matric suction. $\mathbf{T}^{tot}$ is the total stress, u_a is the pore air pressure and u_w is the pore water pressure.

In general, the mechanical behaviour of an unsaturated soil is controlled by a combined effect of the pore air and water pressures in two different ways. First, they control the effective stress (4) in the soil skeleton through an "equivalent pore pressure" u^*, in the same way that the pore water pressure affects the mechanical behaviour of an *equivalent saturated soil*. The equivalent saturated soil will be defined later in the text. Comparison of Eq. (4) with the Terzaghi effective stress equation at saturated conditions ($\mathbf{T} = \mathbf{T}^{tot} - \mathbf{1}u_w$) leads to the following expression of the equivalent pore pressure:

$$u^* = \chi u_w + (1 - \chi)u_a \tag{5}$$

The second effect of the pore air and water in an unsaturated soil is that capillary menisci at the particle contact points generate inter-particle contact forces. These forces differ from the contact forces generated by the boundary forces (quantified by the effective stress (4)) in that their line of action is essentially normal to the plane of contact. An increase of these forces tend to stabilise the contacts and therefore to inhibit grain slippage. This effect is typically manifested by the widely reported stiffened response of the soil skeleton with increasing suction (see, e.g., [9, 20, 28]).

The second effect is conceptually similar to that of chemical bonding of particle contacts in cemented materials. It enables the unsaturated soil, under a given effective stress, to exist at a higher void ratio than the same material at the same effective stress when saturated. In terms of the critical state soil mechanics, the unsaturated soil has a larger SBS and for a given void ratio it has a larger BS.

The state boundary surface and the position of the current state of the soil element with respect to the SBS govern the mechanical behaviour of soil. The mechanical behaviour of an unsaturated soil and the same soil when saturated at the same effective stress and the same void ratio will therefore be significantly different, as the unsaturated soil will have larger BS and therefore it will be apparently more overconsolidated than the saturated soil. In this respect, we define the *equivalent saturated soil* as the soil with the same state (quantified by the effective stress $\mathbf{T}$ and void ratio e) and the same SBS as the unsaturated

soil at the suction level of interest. The *effective stress*[1] *in unsaturated soil* can then be defined as a suitable stress space, in which the soil behaviour is influenced by the relative position of the state to the SBS as in equivalent saturated soil. In turn, the suction controls the size and the shape of the SBS. This definition of the effective stress accords with that of Khalili et al. [20] and it does not exclude straining due to change of suction without the change of effective stress.

A simple formulation for the effective stress tensor **T** based on Eq. (4), which is sufficient for many practical applications, has been put forward by Khalili and Khabbaz [21] and further evaluated by Khalili et al. [20]. On the basis of an extensive evaluation of experimental data they proposed the following empirical formulation for χ:

$$\chi = \begin{cases} 1 & \text{for} \quad s \leq s_e \\ \left(\frac{s_e}{s}\right)^{\gamma} & \text{for} \quad s > s_e \end{cases} \tag{6}$$

where s_e is the suction value separating saturated from unsaturated states. It is equal to the air entry value for the main drying path or the air expulsion value for the main wetting path [20, 28]. γ is a material parameter, and it has been shown that for a broad range of different soils it is sufficient to assign $\gamma = 0.55$ [20, 21]. For suctions lower than s_e the effective stress parameter χ is equal to one, i.e. the soil is saturated and Eq. (4) reduces to the Terzaghi effective stress definition. As stated previously, to avoid undue complication of the theoretical developments and to focus on the application of hypoplasticity to unsaturated soils, hydraulic hysteresis and its impact on the mechanical response of the system has not been considered in the present derivations. Once a general framework for the hypoplasticity of unsaturated soils is established, its extension to include hydraulic hysteresis will be a straightforward matter.

Time differentiation of Eq. (4) with the use of (6) and considering co-rotational terms implies the following formulation of the effective stress rate

$$\mathring{\mathbf{T}} = \mathring{\mathbf{T}}^{net} - \dot{s} \begin{cases} \mathbf{1} & \text{for} \quad s \leq s_e \\ \mathbf{1}(1-\gamma)\chi & \text{for} \quad s > s_e \end{cases} \tag{7}$$

Notice that Eq. (6) is continuous at the saturation-desaturation limit $s = s_e$, whereas the rate of the effective stress $\mathring{\mathbf{T}}$ is not. The discontinuity in the slope of effective stress equation represents the abrupt nature of the desaturation process in porous media. As suction is applied to a saturated soil, it is initially resisted by the surface tension effects at the air-water-solid interface. This trend continues until the point of air entry at which the surface tension at the pores with the largest diameter is overcome and the air enters the void space of the soil in a sudden and discontinuous way.

[1]Some authors prefer to use diffrent terms for **T** in (4), such as *intergranular stress* [19], or *average skeleton stress* [13].

4 Hypoplastic model for unsaturated soils

In this section, the hypoplastic model for saturated soils, outlined briefly in Sec. 2, will be enhanced to predict the behaviour of unsaturated soils. The basic aim is to provide a conceptual way to incorporate the behaviour of unsaturated soils into hypoplasticity. The particular formulation adopted is very simple, but it may be readily modified by using the general rules outlined in this section.

4.1 Model for constant suction

As discussed in Sec. 3, the overall mechanical response of a soil element is controlled by the effective stress. Suction influences the effective stress and in addition it increases normal forces at interparticle contacts and thus acts as a quantity that increases the overall stability of the soil structure. In other words it increases the size of the SBS, in a similar manner to bonding between soil particles in saturated cemented materials.

The incorporation of structure into hypoplastic model has been discussed in detail by Mašín [33, 31]. In this context, the size of the SBS for unsaturated soils is defined by the isotropic virgin compression line which follows from (2)

$$\ln(1+e) = N(s) - \lambda^*(s) \ln \frac{p}{p_r} \tag{8}$$

where e is the void ratio, which is considered as a state variable. Quantities $N(s)$ and $\lambda^*(s)$ define the position and the slope of the isotropic virgin compression line in the $\ln(p/p_r)$ vs. $\ln(1+e)$ plane for given suction s; model parameters N and λ^* then represent their values for saturated conditions (Eq. (2)).

Eq. (8) implies the expression for the Hvorslev equivalent pressure p_e on the isotropic normal compression line for a given suction:

$$p_e = p_r \exp\left[\frac{N(s) - \ln(1+e)}{\lambda^*(s)}\right] \tag{9}$$

Mašín [33] demonstrated that incorporation of variable virgin compressibility and the intercept $N(s)$ into the hypoplastic model requires a modification of both barotropy and pyknotropy factors f_s and f_d in (1). The pyknotropy factor reads

$$f_d = \left(\frac{2p}{p_e}\right)^{\alpha} \tag{10}$$

with p_e calculated according to Eq. (9), and the barotropy factor is given by

$$f_s = -\frac{\mathrm{tr}\mathbf{T}}{\lambda^*(s)} \left(3 + a^2 - 2^{\alpha}\sqrt{3}\right)^{-1} \tag{11}$$

The scalar factor α is still calculated in terms of parameters λ^* and κ^* (see Eq. (45) in Appendix A), to ensure the shape of the BS is not dependent on suction, factor a is given in (45).

4.2 Incorporation of wetting-induced collapse at normally consolidated states

When an unsaturated soil with an initially open structure is subjected to a decreasing suction, the reduction in the normal forces acting at the inter-particle contacts may result in a situation where the structure, for the given effective stress $\mathbf{T}$ and void ratio e, is no longer stable, and thus it collapses. This phenomenon, referred to as wetting-induced collapse, cannot be modelled with the model presented in Sec. 4.1, as $\mathring{\mathbf{T}} = \mathbf{0}$ implies $\mathbf{D} = \mathbf{0}$ (see Eq. (1)), i.e. no deformation of soil skeleton can be predicted for variable suction with constant effective stress.

In the context of the critical state soil mechanics, all admissible states of a soil element are bounded by the SBS. Constant void ratio sections through this surface predicted by the hypoplastic model from Sec. 4.1 have shape independent on e (see Mašín and Herle [34]), the state boundary surface can thus be represented in the stress space normalised by p_e. The stress rate, in the normalised space $\mathbf{T}_n = \mathbf{T}/p_e$, is given by

$$\dot{\mathbf{T}}_n = \frac{\partial}{\partial t}\left(\frac{\mathbf{T}}{p_e}\right) = \frac{\dot{\mathbf{T}}}{p_e} - \frac{\mathbf{T}}{p_e^2}\dot{p}_e \tag{12}$$

The objective (Zaremba-Jaumann, see, e.g., [26]) rate of the normalised stress $\mathring{\mathbf{T}}_n$, which vanishes for rigid body rotation, is given by

$$\mathring{\mathbf{T}}_n = \dot{\mathbf{T}}_n + \mathbf{T}_n \cdot \mathbf{W} - \mathbf{W} \cdot \mathbf{T}_n \tag{13}$$

where the spin tensor $\mathbf{W}$ is the skew-symmetric part of the velocity gradient. Combination of (12) and (13) yields

$$\mathring{\mathbf{T}}_n = \frac{1}{p_e}\left(\dot{\mathbf{T}} + \mathbf{T} \cdot \mathbf{W} - \mathbf{W} \cdot \mathbf{T} - \frac{\mathbf{T}}{p_e}\dot{p}_e\right) = \frac{\mathring{\mathbf{T}}}{p_e} - \frac{\mathbf{T}}{p_e^2}\dot{p}_e \tag{14}$$

The rate of the Hvorslev equivalent stress $\dot{p}_e$ can be found by time-differentiation of Eq. (9) (i.e. comes from Eq. (8) using p_e instead of p)

$$\dot{p}_e = -\frac{p_e}{\lambda^*}\operatorname{tr}\mathbf{D} + \frac{\partial p_e}{\partial s}\dot{s} \tag{15}$$

therefore

$$\mathring{\mathbf{T}}_n = \frac{\mathring{\mathbf{T}}}{p_e} - \frac{\mathbf{T}}{p_e^2}\left(-\frac{p_e}{\lambda^*}\operatorname{tr}\mathbf{D} + \frac{\partial p_e}{\partial s}\dot{s}\right) \tag{16}$$

In this context, the normalised stress rate $\mathring{\mathbf{T}}_n$ will not surpass the state boundary surface if it is coincident with the normalised stress rate $\mathring{\mathbf{T}}_n^{es}$ of an equivalent saturated material (defined in Sec. 3). Note that $\mathring{\mathbf{T}}_n^{es}$ is necessarily bound by the SBS, through its definition. Equivalent saturated material is characterised by $\partial p_e/\partial s = 0$, therefore

$$\mathring{\mathbf{T}}_n^{es} = \frac{1}{p_e}\left(\mathring{\mathbf{T}}^{es} + \frac{\mathbf{T}\operatorname{tr}\mathbf{D}}{\lambda^*}\right) \tag{17}$$

Combination of (16) and (17) yields

$$\mathring{\mathbf{T}} = \mathring{\mathbf{T}}^{es} + \frac{\mathbf{T}}{p_e}\frac{\partial p_e}{\partial s}\dot{s} \tag{18}$$

where $\mathring{\mathbf{T}}^{es}$ is calculated by the hypoplastic model for saturated material (1). Therefore

$$\mathring{\mathbf{T}} = f_s\left(\boldsymbol{\mathcal{L}} : \mathbf{D} + f_d\mathbf{N}\|\mathbf{D}\|\right) + \mathbf{H} \tag{19}$$

where $\mathbf{H}$ is a new term incorporating the collapse of the soil structure due to wetting

$$\mathbf{H} = \frac{\mathbf{T}}{p_e}\frac{\partial p_e}{\partial s}\dot{s} \tag{20}$$

The Hvorslev equivalent pressure p_e is given by Eq. (9), it therefore follows that

$$\mathbf{H} = \frac{\mathbf{T}}{\lambda^*(s)}\left[\frac{\partial N(s)}{\partial s} - \frac{\partial \lambda^*(s)}{\partial s}\ln\frac{p_e}{p_r}\right]\dot{s} \tag{21}$$

4.2.1 Wetting-induced strain rate

Wetting of normally consolidated soil at anisotropic stress state causes in addition to volumetric collapse development of shear strains [45, 46]. Eq. (19) allows us to derive expression for the direction of stretching implied by wetting at constant effective stress for states at the SBS. Eq. (19) for $\mathring{\mathbf{T}} = \mathbf{0}$ reads

$$-\frac{\mathbf{T}}{\lambda^*(s)}\left[\frac{\partial N(s)}{\partial s} - \frac{\partial \lambda^*(s)}{\partial s}\ln\frac{p_e}{p_r}\right]\dot{s} = f_s\left(\boldsymbol{\mathcal{L}} : \mathbf{D} + f_d\mathbf{N}\|\mathbf{D}\|\right) \tag{22}$$

Equation

$$\ln(1+e) = N(s) - \lambda^*(s)\ln\frac{p_e}{p_r} \tag{23}$$

leads after time differentiation to

$$\frac{\dot{e}}{1+e} = \operatorname{tr}\mathbf{D} = \frac{\partial N(s)}{\partial t} - \frac{\partial \lambda^*(s)}{\partial t}\ln\frac{p_e}{p_r} \tag{24}$$

Combination of (22) and (24) yields

$$-\frac{\mathbf{T}}{\lambda^*(s)}\operatorname{tr}\mathbf{D} = f_s\left(\boldsymbol{\mathcal{L}} : \mathbf{D} + f_d\mathbf{N}\|\mathbf{D}\|\right) \tag{25}$$

Eq. (25) has been solved for $\vec{\mathbf{D}}$ in [34]

$$\vec{\mathbf{D}} = -\frac{\boldsymbol{\mathcal{A}}^{-1} : \mathbf{N}}{\|\boldsymbol{\mathcal{A}}^{-1} : \mathbf{N}\|} \tag{26}$$

where the fourth-order tensor $\boldsymbol{\mathcal{A}}$ is given by

$$\boldsymbol{\mathcal{A}} = f_s\boldsymbol{\mathcal{L}} - \frac{1}{\lambda^*(s)}\mathbf{T}\otimes\mathbf{1} \tag{27}$$

Eq. (26) implies purely deviatoric strain rate at the critical state and purely volumetric strain rate at the isotropic stress state. Direction of the strain increment vector for different stress obliquities is graphically demonstrated in Fig. 1, together with the shape of the bounding surface for Pearl clay parameters (Tab. 1), evaluated in Sec. 6.1.

4.3 Model for any state of overconsolidation

The model from Sec. 4.2 may be used for constant value of suction ($\dot{s} = 0$) and for wetting at normally consolidated states (states at the SBS). The following assumptions are utilised to extend Eq. (18) for arbitrary (physically admissible) states and arbitrary loading conditions:

1. As suction controls stability of inter-particle contacts, increasing suction under constant effective stress imposes no deformation of soil skeleton.

2. The more open is the soil structure, the lower is the number of interparticle contacts, so each contact must transmit larger shear forces. When such a structure is wetted under constant effective stress, it will be more prone to collapse than more densely packed structure.

To reflect these two assumptions, the rate formulation of the model is written as

$$\mathring{\mathbf{T}} = f_s \left(\boldsymbol{\mathcal{L}} : \mathbf{D} + f_d \mathbf{N} \|\mathbf{D}\| \right) + f_u \mathbf{H} \tag{28}$$

with

$$\mathbf{H} = -\frac{\mathbf{T}}{\lambda^*(s)} \left[\frac{\partial N(s)}{\partial s} - \frac{\partial \lambda^*(s)}{\partial s} \ln \frac{p_e}{p_r} \right] \langle -\dot{s} \rangle \tag{29}$$

$\langle -\dot{s} \rangle$ is introduced to reflect the first assumption, and f_u, a new pyknotropy factor controlling tendency of the soil structure to collapse upon wetting, to reflect the second.

The factor f_u must be equal to unity for states at the SBS (in that case the structure is as open as possible and collapse is controlled by $\mathbf{H}$ only) and $f_u \to 0$ for $OCR \to \infty$ (no wetting-induced inter-particle slippage occurs in highly overconsolidated soil). The following expression for the factor f_u satisfying these requirements is proposed:

$$f_u = \left(\frac{p}{p^{SBS}} \right)^m \tag{30}$$

where p^{SBS} is the effective mean stress at the SBS corresponding to the current normalised stress $\mathbf{T}/\operatorname{tr}\mathbf{T}$ and current void ratio e and m is a model parameter controlling the influence of overconsolidation on the wetting-induced collapse. From the definition of the pyknotropy factor f_d (Eq. (10)) for $p = p^{SBS}$ follows that

$$\frac{p}{p^{SBS}} = \left(\frac{f_d}{f_d^{SBS}} \right)^{1/\alpha} \tag{31}$$

f_d^{SBS} is the value of the pyknotropy factor f_d at the state boundary surface corresponding to the current state. Analytical expression for f_d^{SBS} has been derived in Reference [34]

$$f_d^{SBS} = \| f_s \boldsymbol{\mathcal{A}}^{-1} : \mathbf{N} \|^{-1} \tag{32}$$

where the fourth-order tensor $\boldsymbol{\mathcal{A}}$ is given by Eq. (27). Therefore, the expression for the pyknotropy factor f_u reads

$$f_u = \left[f_d \| f_s \boldsymbol{\mathcal{A}}^{-1} : \mathbf{N} \| \right]^{m/\alpha} \tag{33}$$

The presented equations define the proposed model under fully general conditions of stress and stretching. As the evaluation of model predictions in Sec. 6 will be often based on isotropic material response, a simpler isotropic formulation of the model has been derived and is given in Appendix B.

5 Calibration of the model

In addition to the parameters of the hypoplastic model for saturated soils (φ_c, N, λ^*, κ^* and r), the proposed model requires quantification of dependency of $N(s)$ and $\lambda^*(s)$ on suction, parameter m that controls the collapse of structure along wetting paths, and suction at air entry and/or air expulsion (s_e).

The general formulation of the model enables to calibrate the functions $N(s)$ and $\lambda^*(s)$ to accommodate the experimental data available through multi-linear or any other higher-order fits, for example in $N(s)$ vs. $\ln(s/s_e)$ and $\lambda^*(s)$ vs. $\ln(s/s_e)$ planes, as shown in Fig 2. In practical applications, however, it is desirable to use formulation with limitted number of material parameters. For the evaluation of model predictions through this paper, we assume for $\ln(s/s_e) > 0$ (unsaturated state)

$$N(s) = N + n \ln\left(\frac{s}{s_e}\right) \qquad\qquad \lambda^*(s) = \lambda^* + l \ln\left(\frac{s}{s_e}\right) \tag{34}$$

The quantities n and l represent two additional soil parameters. The derivatives $\partial N(s)/\partial s$ and $\partial \lambda^*(s)/\partial s$ from Eq. (29) therefore read

$$\frac{\partial N(s)}{\partial s} = \frac{n}{s} \qquad\qquad \frac{\partial \lambda^*(s)}{\partial s} = \frac{l}{s} \tag{35}$$

and the expression for the term $\mathbf{H}$ simplifies to

$$\mathbf{H} = -\mathbf{T} \left[\frac{n - l \ln(p_e/p_r)}{s \lambda^*(s)} \right] \langle -\dot{s} \rangle \tag{36}$$

For $\ln(s/s_e) < 0$ (saturated state) $N(s) = N$ and $\lambda^*(s) = \lambda^*$, i.e. $\partial N(s)/\partial s = 0$, $\partial \lambda^*(s)/\partial s = 0$ and therefore $\mathbf{H} = \mathbf{0}$.

The parameter m defines the rate at which susceptibility of the structure to collapse decreases with increasing distance from the state boundary surface. The Eq. (30) is graphically represented in Fig. 3. For $m \to \infty$ the model predicts collapsible strains for states at the state boundary surface only, i.e. predictions of wetting-induced collapse then correspond to predictions by single-surface elasto-plastic models (such as [28]). With decreasing m, the collapsible strains occur also inside the SBS, similarly to predictions by multi-surface kinematic hardening or bounding surface plasticity models (e.g., [42]).

The influence of the parameter m on predictions of wetting test at constant net stress on slightly overconsolidated soil is shown in Fig. 4c. This figure demonstrates calibration of the parameter m by means of experimental data on Pearl clay [45, 46], which will be used in Sec. 6 for evaluation of the model predictions. For high values of m the collapse of structure begins abruptly when the state reaches SBS, inside the SBS swelling caused by decrease of the effective stress is predicted. For lower values of m the collapse takes place further from the SBS and for m approaching one the collapse of the structure for this particular situation occurs since the beginning of the wetting test. The parameter m can be calibrated by means of a parametric study using wetting test on slightly overconsolidated soil, such as the one in Fig. 4c. Its calibration requires the knowledge of the soil behaviour inside the SBS and of the shape of the SBS, therefore all other soil parameters should be known before m is calibrated. It is important to point out that all model parameters with the exception of m (and obviously s_e) may be found by means of laboratory experiments at constant value of suction.

The last parameter s_e controls the formulation of the effective stress and its calibration has been thoroughly discussed by Khalili and Khabbaz [21] and Khalili et al. [20]. As already mentioned, the formulation adopted by Khalili and Khabbaz [21] does not take into account the influence of hydraulic hysteresis, therefore s_e must be calibrated to represent the air-entry value for wetting processes and the air expulsion value for drying processes. As these values may differ quite substantially, the parameter s_e is calibrated by considering which process is of the particular interest in a situation where the model will be applied, having in mind that eventual predictions of the opposite process with the same parameters would be less accurate.

6 Evaluation of the model

The experimental data used for the evaluation of the model predictions have been chosen in order to evaluate different aspects of the constitutive model formulation. The behaviour of soils with different apparent overconsolidation ratios (OCR, defined here as $OCR = p_e/p$) along wetting paths is evaluated by means of experiments on Pearl clay by Sun et al. [45, 46]. Tests on White clay, Orly loam and Sterrebeek loam by Fleureau et al. [12] allow studying the model response to drying paths. Finally, the set of data on Jossigny silt by Cui and Delage [9] is used to evaluate predictions of shear tests at constant suction on soils with different apparent OCRs.

6.1 Response to wetting paths

Evaluation of the response of the proposed model to wetting path is important as in this case the term **H** and the pyknotropy factor f_u, novel in hypoplasticity, are activated. The model is evaluated by means of experimental data on statically compacted Pearl clay by Sun et al. [45, 46]. Pearl clay is a moderate plasticity soil with very little expansive clay minerals.

Experimental results from the following tests will be used for the model evaluation. In the first set of data, the specimens have been isotropically compressed at constant suction 147 kPa to different mean net stress levels (20, 49, 98, 196, 392 and 588 kPa). At this stage, the specimens were wetted and suction was decreased to zero. Volumetric strains for different suction levels were logged during suction reduction. Some of the specimens were further compressed at zero suction to the mean net stress 588 kPa.

To investigate the influence of the stress anisotropy on the wetting-induced collapse behaviour, other specimens, after isotropic compression at constant suction $s = 147$ kPa to mean net stress $p^{net} = 196$ kPa, were subjected to constant suction and constant p^{net} stress paths up to a target principal net stress ratio $R = T_a^{net}/T_r^{net}$, where T_a^{net} and T_r^{net} are the axial and radial net stresses. At this stage, suction was decreased to zero under constant net stress and finally the shear test continued under constant p^{net} and $s = 0$ kPa to failure. Three respective sets of experimental data will be used for the model evaluation - in the first one four specimens with different initial void ratios have been wetted at $R = 1.5$, so the influence of the apparent OCR on wetting at anisotropic stress state could be investigated. In the second set three specimens with approximately equal initial void ratios are wetted at different values of the ratio R (1.5, 2 and 2.5) and sheared in compression, the third set is equivalent (with $R = 1.5$, 2 and 2.2), but the samples were sheared in extension.

As the wetting process is of the primary interest in this set of experimental data, the parameter s_e represents the suction at air expulsion. Its value has been estimated from the degree of saturation S_r vs. s graphs provided by Sun et al. [46]. They range from 2 to 30 kPa. An approximate average value of 15 kPa is adopted. The parameters N, λ^*, n and l are obtained from the isotropic compression paths at $s = 147$ kPa and $s = 0$ kPa. Their calibration is demonstrated in Fig. 4a, which shows the effective stress paths of the five isotropic compression experiments at two suction levels and indicates the assumed normal compression lines. The parameter κ^* has been found using the experiments at $s = 147$ kPa to predict correctly the slope of the isotropic compression line of the initially apparently overconsolidated specimens, see Fig. 4b. The parameter m has been found by simulating the wetting test at the high apparent overconsolidation ratio (the test where wetting took place at $p^{net} = 49$ kPa), see Fig. 3b. The parameter φ_c (critical state friction angle) has been found using standard procedure by evaluation of triaxial shear test data and r (factor controlling the shear stiffness) has been found by means of simulation of the constant p^{net} shear test, as shown in Fig. 4d. The whole set of material parameters on Pearl clay is given in Tab. 1.

Figures 5 – 9 show simulations of different tests on Pearl clay by Sun et al. [45, 46]. Experiments which have been used for calibration of model parameters are indicated by labels in the figures, in all other cases the graphs show model predictions. Figure 5 shows paths of the constant suction isotropic compression tests and constant net stress wetting tests replotted in the effective stress space, experimental data are compared with predictions by the proposed model. The model predicts correctly both the constant suction and wetting parts of the experiments. In the wetting tests at the lower net mean stresses, the experiments show the initial decrease of the effective stress with very small change of void ratio. This aspect of the observed soil behaviour, which is progressively less pronounced

with decreasing apparent OCR, can be modelled correctly by the proposed model thanks to the factor f_u.

Results of the wetting parts of the experiments from Fig. 5 in the suction vs. volumetric strain plane are plotted in Fig. 6. The model predicts correctly the qualitative influence of the net mean stress on the volumetric behaviour. When the soil is wetted at a low p^{net} (20 and 49 kPa), it first swells and only after the state gets closer to the state boundary surface the structure starts to collapse. On the other hand, specimens wetted at higher net mean stresses (i.e. at lower apparent OCRs) collapse since the beginning of the wetting test. Modelling of this aspect of the soil behaviour is, again, enabled by the factor f_u. The experiments show the lowest collapsible strains for the wetting at the highest net mean stress (588 kPa). Correct predictions of the final value of the volumetric strains after collapse are achieved thanks to the converging normal compression lines of the saturated and unsaturated soils (Figs. 4a, 5). The predicted shape of the wetting path in the s vs. ϵ_v plane is controlled by the factor f_u (for the initially apparently overconsolidated specimens) and by the interpolation function for the quantities $N(s)$ and $\lambda^*(s)$. Good agreement between experimental data and model predictions also for wetting at higher net mean stresses (where the factor f_u takes a constant value equal to one) suggests that the logarithmic interpolation adopted (Eq. (34)) is suitable to represent the Pearl clay behaviour. The predicted volumetric strain curve changes abruptly as the suction reaches the air expulsion value. The soil becomes at lower suctions effectively saturated and the model then predicts swelling caused by decrease of the effective stress.

Figures 7a and 7b show ϵ_a vs. R and ϵ_a vs. ϵ_v graphs of the constant net mean stress shear tests and constant $R = 1.5$ wetting tests with different initial void ratios (different initial apparent OCRs). Both the constant suction R vs. ϵ_a response and the increasing tendency to collapse (in terms of both ϵ_v and ϵ_a) for increasing initial void ratio (decreasing apparent OCR) are predicted satisfactorily. The only qualitative discrepancy is in that the model does not predict dilatant behaviour of the initially densest specimen in the constant p^{net} stress after wetting.

Figure 8a shows the results of the three constant net mean stress compression shear tests in the axial strain vs. principal net stress ratio plane, and Figure 9c similar experiments in triaxial extension. The specimens had approximately equal initial void ratios (initial apparent OCRs) and wetting took place at different values of the ratio R. The corresponding volumetric behaviour is in Figs. 8b and 9b and radial strains in Figs. 8c and 9a. Predictions of the constant suction parts of the tests, reasonable at least from the qualitative point view, demonstrate the predictive capabilities of the basic hypoplastic model. In the wetting parts of the tests, the model predicts approximately equal collapse volumetric strains and significant increase of the absolute values of collapse axial and radial strains at higher ratios R. The good quantitative agreement for both ϵ_a and ϵ_r demonstrates adequate modelling of the wetting-induced collapse strain rate direction. The analytical expression for this direction has been (for constant effective stress) derived in Sec. 4.2.1, see Fig. 1 for Pearl clay parameters.

6.2 Response to drying paths

To study the response of the model to drying paths, laboratory experiments on three different soils by Fleureau et al. [12] have been simulated. The drying tests have been performed on initially saturated remolded samples, either directly from the slurry state at a water content w equal to 1.5 times the liquid limit w_L, or on specimens consolidated from the slurry in an oedometer under different vertical stresses. As the range of applied suctions was very wide, it has been controlled be several techniques, including tensiometric plate (suction 0 kPa to 20 kPa), air pressure control and osmotic technique (50 kPa to 1500 kPa) and relative humidity control using salt solutions for high suction levels (2 MPa to 1000 MPa). The authors demonstrated that the techniques used gave consistent results. As only limitted amount of data is available for each soil, the parameters have been found by means of simulation of test data presented only and results in Fig. 10 therefore do not represent pure predictions. Nonetheless, they still demonstrate some capabilities of the proposed model. All model parameters used are summarised in Tab. 1.

Figure 10a shows results of drying paths on Orly loam on two specimens: one dried from a slurry state and the other preconsolidated in an oedometer at a net vertical stress -100 kPa. As the reconstituted Orly loam has a very high air entry value of suction (4000 kPa), the two specimens reached normally consolidated state at suctions lower than s_e and with continued drying their response coincide. When the suction reaches the air entry value abrupt change of soil behaviour is observed, the soil structure stiffens significantly and very little change in void ratio is observed with further suction increase. This observed behaviour is represented well by the proposed hypoplastic model. For suctions lower than s_e predictions correspond to the reference hypoplastic model for saturated materials. However, when the suction reaches the air entry value, the SBS starts to increase in size rapidly, which leads to very stiff behaviour with further drying.

The same experiments have been performed on Sterrebeek loam (Figure 10b), with the exception that the consolidated sample has been preloaded to higher net vertical stress (-200 kPa). The observed behaviour is, however, significantly different as compared to the response of Orly loam. As Sterrebeek loam has significantly lower air entry value, the consolidated sample became unsaturated before it reached the normally consolidated state. The sample is therefore relatively stiff in the saturated region and less pronounced change of stiffness is observed when the unsaturated state is reached. Also this type of behaviour can be well simulated by the proposed model.

Finally, Fig. 10c shows response of the white clay (kaolin) to the drying-wetting cycle. As the white clay has very small hydraulic hysteresis and the air entry and air expulsion values are similar, the model is capable of simulating both the drying and wetting behaviour of this soil with a single set of material parameters. The model simulates lower stiffness in the saturated than in unsaturated region. The stiffness in the saturated region is significantly lower for drying than for wetting process.

6.3 Response at constant suction

Cui and Delage [9] performed a series of drained triaxial tests on an aeolian silt from Jossigny near Paris. The soil has been statically compacted and isotropically compressed under four different applied suction levels (200, 400, 800 and 1500 kPa). The isotropic compression has been terminated at five different p^{net} levels (50, 100, 200, 400 and 600 kPa) and followed by a drained triaxial compression test. Therefore, all together twenty shear tests on soils with different apparent OCRs have been performed, with apparent OCR increasing with suction and decreasing with net cell pressure.

The air-entry value s_e of the compacted Jossigny loam has been taken from Khalili et al. [20]. As the set of experimental data does not include tests on saturated soils, the parameter λ^* has been calibrated using isotropic compression test at $s = 200$ kPa and $l = 0$ has been assumed. The parameters N, n and κ^* have then been evaluated by a trial-and-error procedure in order to reproduce the stress-dilatancy behaviour of the shear tests. Parameters φ_c and r have been found using standard approach as outlined in [30]. The parameter m has not been not evaluated, as no tests with decreasing suction were simulated so m is not needed in simulations. All parameters used in evaluation are given in Tab. 1. Similarly to tests with drying paths, results in Fig. 11 have all been used for evaluation of model parameters, they therefore represent simulations, rather than pure predictions by the proposed model.

Figure 11(a) shows the deviatoric stress vs. shear strain curves of the tests analysed and Figure 11(b) shows the corresponding volumetric behaviour. The proposed model gives qualitatively good predictions, taking into account that the tests were performed at four different suction levels, while the influence of suction on the apparent OCR is characterised by a single material parameter n (recall that change of $\lambda^*(s)$ is not considered here, i.e. $l = 0$). As observed in the experiments, the model predicts increase of the maximum deviator stress with both the suction and the cell pressure. Also, for a given cell pressure, both experimental data and simulations show decreasing tendency for volumetric contractancy with increasing suction. For low cell pressures and high suctions the model predicts dilatant behaviour and a peak in the deviatoric stress vs. shear strain curve. Similar behaviour is observed in the experiments, although the agreement is not perfect from a quantitative point of view.

7 Summary and conclusions

A new hypoplastic model for unsaturated soils, based on the effective stress concept with a scalar quantity that describes stiffening of the soil structure, has been proposed. The formulation combines the mathematically simple hypoplastic model by Mašín [30] with the effective stress equation by Khalili and Khabbaz [21]. These two approaches have been chosen as they require only limited number of material parameters, so they yield a model easy for use in practical applications.

A new method for incorporating the wetting-induced collapse into hypoplasticity has been proposed in the paper. The approach yields new tensorial term **H** entering the hy-

poplastic equation, which is calculated through the requirement of consistency on the state boundary surface. Further, new pyknotropy factor f_u is proposed in order to simulate different response of soils with different apparent overconsolidation.

Evaluation of the model predictions has been based on a number of experimental data sets, performed on different soils in different soil mechanics laboratories. Although the complete model requires only nine material parameters with a clear physical interpretation, it can predict reasonably a number different aspects of unsaturated soil behaviour, namely

1. Response of normally consolidated and apparently overconsolidated soils to wetting paths. Model predicts wetting-induced collapse of normally consolidated soils, swelling of highly overconsolidated soils and a smooth transition between the two cases, controlled by the new constitutive parameter m. Also, the model predicts the influence of the stress ratio on the behaviour upon wetting.

2. Response of normally consolidated and apparently overconsolidated soils to drying paths. The model predicts stiffening of the soil response at suction at air entry, where the soil starts to be effectively unsaturated. Different responses before and after air entry can be modelled quantitatively with a single set of material parameters.

3. Response of normally consolidated and apparently overconsolidated soils to shear tests performed at constant suction. Suction influences the size of the state boundary surface and it thus controls the predicted peak friction angle and the stress-dilatancy relationship.

The predicted soil response is non-linear also in the overconsolidated state. To this respect, the model provides a qualitative advance with respect to many existing constitutive models for mechanical response of unsaturated soils.

Acknowledgment

The first author acknowledges the financial support by the research grants GAAV IAA200710605, GACR 103/07/0678 and MSM0021620855.

Appendix A

The appendix A summarises mathematical formulation of the reference hypoplastic model for saturated soils [30]. The constitutive equation in rate form reads:

$$\mathring{\mathbf{T}} = f_s \boldsymbol{\mathcal{L}} : \mathbf{D} + f_s f_d \mathbf{N} \|\mathbf{D}\| \tag{37}$$

where:

$$\boldsymbol{\mathcal{L}} = 3\left(c_1 \boldsymbol{\mathcal{I}} + c_2 a^2 \hat{\mathbf{T}} \otimes \hat{\mathbf{T}}\right) \qquad \mathbf{N} = \boldsymbol{\mathcal{L}} : \left(-Y \frac{\mathbf{m}}{\|\mathbf{m}\|}\right) \qquad \hat{\mathbf{T}} = \frac{\mathbf{T}}{\operatorname{tr} \mathbf{T}} \tag{38}$$

$\mathbf{1}$ is the second–order identity tensor and $\boldsymbol{\mathcal{I}}$ is the fourth–order identity tensor, with components:

$$(\mathcal{I})_{ijkl} = \frac{1}{2}\left(1_{ik}1_{jl} + 1_{il}1_{jk}\right) \tag{39}$$

In eq. (37), the functions $f_s(\mathrm{tr}\,\mathbf{T})$ (*barotropy* factor) and $f_d(\mathrm{tr}\,\mathbf{T}, e)$ (*pyknotropy* factor) are given by:

$$f_s = -\frac{\mathrm{tr}\mathbf{T}}{\lambda^*}\left(3 + a^2 - 2^\alpha a\sqrt{3}\right)^{-1} \qquad f_d = \left[-\frac{2\mathrm{tr}\mathbf{T}}{3p_r}\exp\left(\frac{\ln(1+e) - N}{\lambda^*}\right)\right]^\alpha \tag{40}$$

where p_r is the reference stress 1 kPa. The scalar function Y and the second–order tensor $\mathbf{m}$ appearing in Eq. (38) are given, respectively, by:

$$Y = \left(\frac{\sqrt{3}a}{3+a^2} - 1\right)\frac{(I_1 I_2 + 9I_3)\left(1 - \sin^2\varphi_c\right)}{8I_3\sin^2\varphi_c} + \frac{\sqrt{3}a}{3+a^2} \tag{41}$$

in which:

$$I_1 = \mathrm{tr}\mathbf{T} \qquad I_2 = \frac{1}{2}\left[\mathbf{T}:\mathbf{T} - (I_1)^2\right] \qquad I_3 = \det\mathbf{T}$$

and

$$\mathbf{m} = -\frac{a}{F}\left[\hat{\mathbf{T}} + \hat{\mathbf{T}}^* - \frac{\hat{\mathbf{T}}}{3}\left(\frac{6\,\hat{\mathbf{T}}:\hat{\mathbf{T}} - 1}{(F/a)^2 + \hat{\mathbf{T}}:\hat{\mathbf{T}}}\right)\right] \tag{42}$$

in which:

$$\hat{\mathbf{T}}^* = \hat{\mathbf{T}} - \frac{\mathbf{1}}{3} \qquad F = \sqrt{\frac{1}{8}\tan^2\psi + \frac{2 - \tan^2\psi}{2 + \sqrt{2}\tan\psi\cos 3\theta}} - \frac{1}{2\sqrt{2}}\tan\psi \tag{43}$$

$$\tan\psi = \sqrt{3}\|\hat{\mathbf{T}}^*\| \qquad \cos 3\theta = -\sqrt{6}\frac{\mathrm{tr}\left(\hat{\mathbf{T}}^*\cdot\hat{\mathbf{T}}^*\cdot\hat{\mathbf{T}}^*\right)}{\left(\hat{\mathbf{T}}^*:\hat{\mathbf{T}}^*\right)^{3/2}} \tag{44}$$

Finally, the scalars a, α, c_1 and c_2 appearing in eqs. (38)–(42), are given as functions of the material parameters φ_c, λ^*, κ^* and r by the following relations:

$$a = \frac{\sqrt{3}\,(3 - \sin\varphi_c)}{2\sqrt{2}\sin\varphi_c} \qquad \alpha = \frac{1}{\ln 2}\ln\left[\frac{\lambda^* - \kappa^*}{\lambda^* + \kappa^*}\left(\frac{3+a^2}{a\sqrt{3}}\right)\right] \tag{45}$$

$$c_1 = \frac{2\left(3 + a^2 - 2^\alpha a\sqrt{3}\right)}{9r} \qquad c_2 = 1 + (1 - c_1)\frac{3}{a^2} \tag{46}$$

The model requires five constitutive parameters, namely φ_c, λ^*, κ^*, N and r, state is characterised by the Cauchy stress $\mathbf{T}$ and void ratio e.

Appendix B

This Appendix presents an isotropic formulation of the proposed hypoplastic model. The effective stress is quantified by mean stress $p = -\operatorname{tr}\mathbf{T}/3$, stretching by the rate of void ratio $\dot{e} = \operatorname{tr}\mathbf{D}(1+e)$. The effective stress rate predicted by the proposed model is given by Eqs. (18), (28) and (29)

$$\mathring{\mathbf{T}} = \mathring{\mathbf{T}}^{es} - f_u \frac{\mathbf{T}}{p_e}\frac{\partial p_e}{\partial s}\langle -\dot{s}\rangle \tag{47}$$

where the Hvorslev equivalent stress p_e is given by Eq. (9), suction s is a state variable and f_u is a pyknotropy factor from Eq. (30). It follows that

$$\dot{p} = -\frac{\operatorname{tr}\mathring{\mathbf{T}}}{3} = -\frac{\operatorname{tr}\mathring{\mathbf{T}}^{es}}{3} + f_u\frac{\operatorname{tr}\mathbf{T}}{3p_e}\frac{\partial p_e}{\partial s}\langle -\dot{s}\rangle = -\frac{\operatorname{tr}\mathring{\mathbf{T}}^{es}}{3} - f_u\frac{p}{p_e}\frac{\partial p_e}{\partial s}\langle -\dot{s}\rangle \tag{48}$$

An isotropic formulation of the quantity $-\operatorname{tr}\mathring{\mathbf{T}}^{es}/3$ has been derived in Reference [30], we thus have the following isotropic form of the proposed hypoplastic model:

$$\dot{p} = -\frac{1}{3\,(1+e)} f_s\left[\left(3+a^2\right)\dot{e} + f_d a\sqrt{3}|\dot{e}|\right] - f_u\frac{p}{p_e}\frac{\partial p_e}{\partial s}\langle -\dot{s}\rangle \tag{49}$$

The scalar quantity a has been defined in (45) and the barotropy factor f_s in Eq. (11). Its isotropic formulation reads

$$f_s = \frac{3p}{\lambda^*(s)}\left(3 + a^2 - 2^\alpha\sqrt{3}\right)^{-1} \tag{50}$$

where the quantity α is given in Eq. (45). An isotropic formulation of pyknotropy factors f_d and f_u read (see (10) and (30))

$$f_d = \left(\frac{2p}{p_e}\right)^\alpha \qquad\qquad f_u = \left(\frac{p}{p_e}\right)^m \tag{51}$$

In Eqs. (49) – (51) p, e and s are state variables, m is a model parameter and all other quantities can be calculated in terms model parameters N, λ^*, κ^*, φ_c, n, l and s_e.

References

[1] E. Alonso, A. Gens, and A. Josa. A constitutive model for partially saturated soils. *Géotechnique*, 40(3):405–430, 1990.

[2] E. Bauer, W. Cen, Y. Zhu, K. Kast, and S. F. Tantono. Modelling of partly saturated weathered broken rock. In H. F. Schweiger, editor, *Proc. 6^{th} European Conference on Numerical Methods in Geomechanics (NUMGE06), Graz, Austria*, pages 87–92. Taylor & Francis Group, London, 2006.

[3] E. Bauer, S. F. Tantono, W. Cen, Y. Zhu, and K. Kast. Hypoplastic modelling of the disintegration of dry saturated weathered broken rock. In T. Schanz, editor, *Theoretical and numerical unsaturated soil mechanics*, pages 11–18. Springer-Verlag Berlin Heidelberg, 2007.

[4] A. W. Bishop. The principle of effective stress. *Teknisk Ukeblad*, 106(39):859–863, 1959.

[5] G. Bolzon, A. Schrefler, and O. C. Zienkiewicz. Elasto-plastic constitutive laws generalised to partially saturated states. *Géotechnique*, 46(2):279–289, 1996.

[6] R. I. Borja. Cam–clay plasticity, Part V: A mathematical framework for three-phase deformation and strain localzation analyses of partially saturated porous media. *Comp. Meth. Appl. Mech. Engng.*, 193:5301–5338, 2004.

[7] R. Butterfield. A natural compression law for soils. *Géotechnique*, 29(4):469–480, 1979.

[8] R. Chambon. Une classe de lois de comportement incrémentalement nonlináires pour les sols non visqueux, résolution de quelques problèmes de cohérence. *C. R. Acad. Sci.*, 308(II):1571–1576, 1989.

[9] Y. J. Cui and P. Delage. Yielding and plastic behaviour of an unsaturated compacted silt. *Géotechnique*, 46(2):291–311, 1996.

[10] W. Ehlers, T. Graf, and M. Ammann. Deformation and localization analysis of partially saturated soil. *Comp. Meth. Appl. Mech. Engng.*, 193:2885–2910, 2004.

[11] W. Fellin and A. Ostermann. Consistent tangent operators for constitutive rate equations. *International Journal for Numerical and Analytical Methods in Geomechanics*, 26:1213–1233, 2002.

[12] J.-M. Fleureau, S. Kheirbek-Saoud, R. Soemitro, and S. Taibi. Behaviour of clayey soils on drying-wetting paths. *Canadian Geotechnical Journal*, 30(2):287–296, 1993.

[13] D. Gallipoli, A. Gens, R. Sharma, and J. Vaunat. An elasto-plastic model for unsaturated soil incorporating the effects of suction and degree of saturation on mechanical behaviour. *Géotechnique*, 53(1):123–135, 2003.

[14] G. Gudehus. A comprehensive concept for non-saturated granular bodies. In Alonso and Delage, editors, 1^{st} *Int. Conference on Unsaturated Soils, Paris, France*, volume 2, pages 725–737. Balkema, Rotterdam, 1995.

[15] G. Gudehus. A comprehensive constitutive equation for granular materials. *Soils and Foundations*, 36(1):1–12, 1996.

[16] G. Gudehus. A visco-hypoplastic constitutive relation for soft soils. *Soils and Foundations*, 44(4):11–25, 2004.

[17] V. Hájek and D. Mašín. An evaluation of constitutive models to predict the behaviour of fine-grained soils with different degrees of overconsolidation. In H. F. Schweiger, editor, *Proc. 6th European Conference on Numerical Methods in Geomechanics (NUMGE06), Graz, Austria*, pages 49–55. Taylor & Francis Group, London, 2006.

[18] I. Herle and D. Kolymbas. Hypoplasticity for soils with low friction angles. *Computers and Geotechnics*, 31(5):365–373, 2004.

[19] J. E. B. Jennings and J. B. Burland. Limitations to the use of effective stresses in saturated soils. *Géotechnique*, 12(2):125–144, 1962.

[20] N. Khalili, F. Geiser, and G. E. Blight. Effective stress in unsaturated soils: review with new evidence. *International Journal of Geomechanics*, 4(2):115–126, 2004.

[21] N. Khalili and M. H. Khabbaz. A unique relationship for χ for the determination of the shear strength of unsaturated soils. *Géotechnique*, 48(2):1–7, 1998.

[22] N. Khalili and B. Loret. An elasto-plastic model for non-isothermal analysis of flow and deformation in unsaturated porous media: formulation. *International Journal of Solids and Structures*, 38:8305–8330, 2001.

[23] Y. Kogho, M. Nakano, and T. Myazaki. Theoretical aspects of constitutive modeling for unsaturated soils. *Soils and Foundations*, 33(4):49–63, 1993.

[24] D. Kolymbas. Computer-aided design of constitutive laws. *International Journal for Numerical and Analytical Methods in Geomechanics*, 15:593–604, 1991.

[25] D. Kolymbas. An outline of hypoplasticity. *Archive of Applied Mechanics*, 61:143–151, 1991.

[26] D. Kolymbas and I. Herle. Shear and objective stress rates in hypoplasticity. *International Journal for Numerical and Analytical Methods in Geomechanics*, 27:733–744, 2003.

[27] B. Loret and N. Khalili. A three-phase model for unsaturated soils. *International Journal for Numerical and Analytical Methods in Geomechanics*, 24:893–927, 2000.

[28] B. Loret and N. Khalili. An effective stress elastic-plastic model for unsaturated porous media. *Mechanics of Materials*, 34:97–116, 2002.

[29] H. Matsuoka and T. Nakai. Stress–deformation and strength characteristics of soil under three different principal stresses. In *Proc. Japanese Soc. of Civil Engineers*, volume 232, pages 59–70, 1974.

[30] D. Mašín. A hypoplastic constitutive model for clays. *International Journal for Numerical and Analytical Methods in Geomechanics*, 29(4):311–336, 2005.

[31] D. Mašín. Incorporation of meta-stable structure into hypoplasticity. In *Proc. Int. Conference on Numerical Simulation of Construction Processes in Geotechnical Engineering for Urban Environment*, pages 283–290. Bochum, Germany, 2006.

[32] D. Mašín. Comparison of elasto-plastic and hypoplastic modelling of structured clays. In J.-H. Yin, X. S. Li, A. T. Yeung, and C. S. Desai, editors, *Proc. International Workshop on Constitutive Modelling - Development, Implementation, Evaluation, and Application*, pages 387–392. Hong Kong, China, 2007.

[33] D. Mašín. A hypoplastic constitutive model for clays with meta-stable structure. *Canadian Geotechnical Journal*, 44(3):363–375, 2007.

[34] D. Mašín and I. Herle. State boundary surface of a hypoplastic model for clays. *Computers and Geotechnics*, 32(6):400–410, 2005.

[35] D. Mašín, C. Tamagnini, G. Viggiani, and D. Costanzo. Directional response of a reconstituted fine grained soil. Part II: performance of different constitutive models. *International Journal for Numerical and Analytical Methods in Geomechanics*, 30(13):1303–1336, 2006.

[36] A. Modaressi and N. Abou-Bekr. A unified approach to model the behavior of saturated and unsaturated soils. In H. J. Siriwardane and M. M. Zaman, editors, *Proc. 8^{th} Int. Conference IACMAG*, pages 1507–1513. Balkema, 1994.

[37] A. Niemunis. A visco-plastic model for clay and its FE implementation. In E. Dembicki, W. Cichy, and L. Balachowski, editors, *Recent results in mechanics of soils and rocks.*, pages 151–162. TU Gdańsk, 1996.

[38] A. Niemunis. *Extended hypoplastic models for soils*. Habilitation thesis, Ruhr-University, Bochum, 2002.

[39] A. Niemunis. Anisotropic effects in hypoplasticity. In Di Benedetto et al., editor, *Deformation Characteristics of Geomaterials*, pages 1211–1217, 2003.

[40] A. Niemunis and I. Herle. Hypoplastic model for cohesionless soils with elastic strain range. *Mechanics of Cohesive-Frictional Materials*, 2:279–299, 1997.

[41] K. H. Roscoe and J. B. Burland. On the generalised stress-strain behaviour of wet clay. In J. Heyman and F. A. Leckie, editors, *Engineering Plasticity*, pages 535–609. Cambridge: Cambridge Univesrity Press, 1968.

[42] A. R. Russell and N. Khalili. A unified bounding surface plasticity model for unsaturated soils. *International Journal for Numerical and Analytical Methods in Geomechanics*, 30(3):181–212, 2006.

[43] R. Santagiuliana and B. A. Schrefler. Enhancing the Bolzon-Schrefler-Zienkiewicz constitutive model for partially saturated soil. *Transport in Porous Media*, 65(1):1–30, 2006.

[44] D. Sheng, S. W. Sloan, and A. Gens. A constitutive model for unsaturated soils: thermomechanical and computational aspects. *Computational Mechanics*, 33(6):453–465, 2004.

[45] D. A. Sun, H. Matsuoka, and Y. F. Xu. Collapse behaviour of compacted clays in suction-controlled triaxial tests. *Geotechnical Testing Journal*, 27(4):362–370, 2004.

[46] D. A. Sun, D. Sheng, and Y. F. Xu. Collapse behaviour of unsaturated compacted soil with different initial densities. *Canadian Geotechnical Journal*, 44(6):673–686, 2007.

[47] C. Tamagnini, D. Mašín, D. Costanzo, and G. Viggiani. An evaluation of different constitutive models to predict the directional response of a reconstituted fine-grained soils. In W. Wu and H. S. Yu, editors, *Proc. Int. workshop Modern trends in geomechanics, Vienna, Austria*, pages 143–157. Springer, Berlin, 2005.

[48] J. Vaunat, E. Romero, and C. Jommi. An elastoplastic hydro-mechanical model for unsaturated soil. In *Experimental Evidence and Theoretical Approaches in Unsaturated Soils, Proc. of Int. Workshop on Unsaturated Soil, Trento, Italy*, pages 121–137. Balkema, Rotterdam, 2000.

[49] P. A. von Wolffersdorff. A hypoplastic relation for granular materials with a predefined limit state surface. *Mechanics of Cohesive-Frictional Materials*, 1:251–271, 1996.

[50] S. Wheeler and V. Sivakumar. An elasto-plastic critical state framework for unsaturated soils. *Géotechnique*, 45(1):35–53, 1995.

[51] S. J. Wheeler, R. S. Sharma, and M. S. R. Buisson. Coupling of hydraulic hysteresis and stress-strain behaviour in unsaturated soils. *Géotechnique*, 53:41–54, 2003.

[52] W. Wu. Rational approach to anisotropy of sand. *International Journal for Numerical and Analytical Methods in Geomechanics*, 22:921–940, 1998.

[53] W. Wu and W. Huang. Rational approach to anisotropy of rocks. In *Proc. EUROCK Symposium*, pages 623–628. Aachen, Germany, 2000.

Table 1: *Parameters of proposed hypoplastic model for soils investigated. Values in brackets have only been estimated, they do not have substantial effects on presented simulations.*

	φ_c	λ^*	κ^*	N	r	n	l	m	s_e [kPa]
Pearl clay [45, 46]	29°	0.05	0.005	1.003	0.5	0.164	0.024	2	15 (expulsion)
White clay (kaolin) [12]	(22°)	0.077	0.008	1.25	n/a	(0.1)	(0)	(10)	1900 (ent. & exp.)
Orly loam [12]	(25°)	0.053	0.005	0.785	n/a	(0.1)	(0)	n/a	4000 (entry)
Sterrebeek loam [12]	(25°)	0.022	0.005	0.58	n/a	(0.1)	(0)	n/a	90 (entry)
Jossigny silt [9]	25°	0.04	0.005	0.72	0.5	0.025	0	n/a	185 (entry)

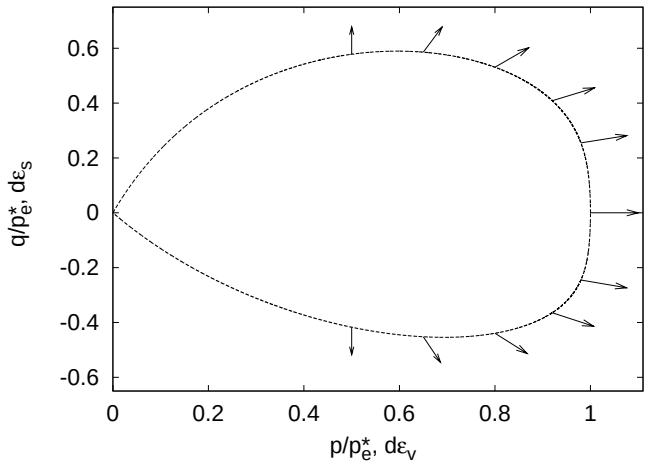

Figure 1: Direction of strain rate tensor induced by wetting at constant effective stress for Pearl clay parameters.

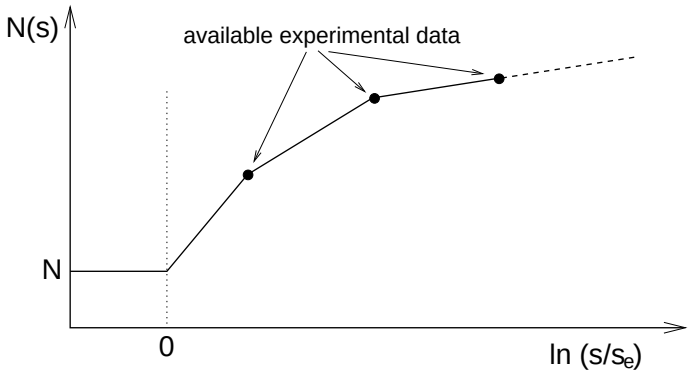

Figure 2: Multi-linear diagram for calibration of the quantity $N(s)$ by means of all experimental data available.

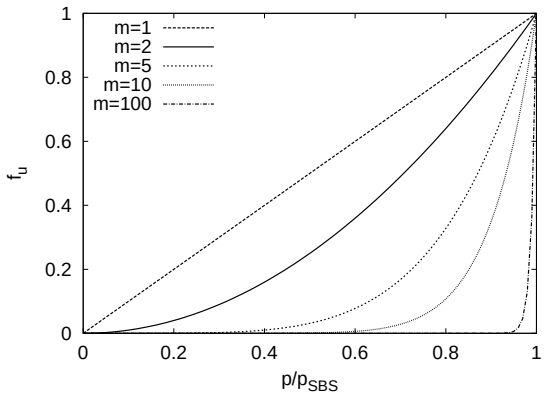

Figure 3: The influence of the parameter m on the value of suction a new pyknotropy factor f_u.

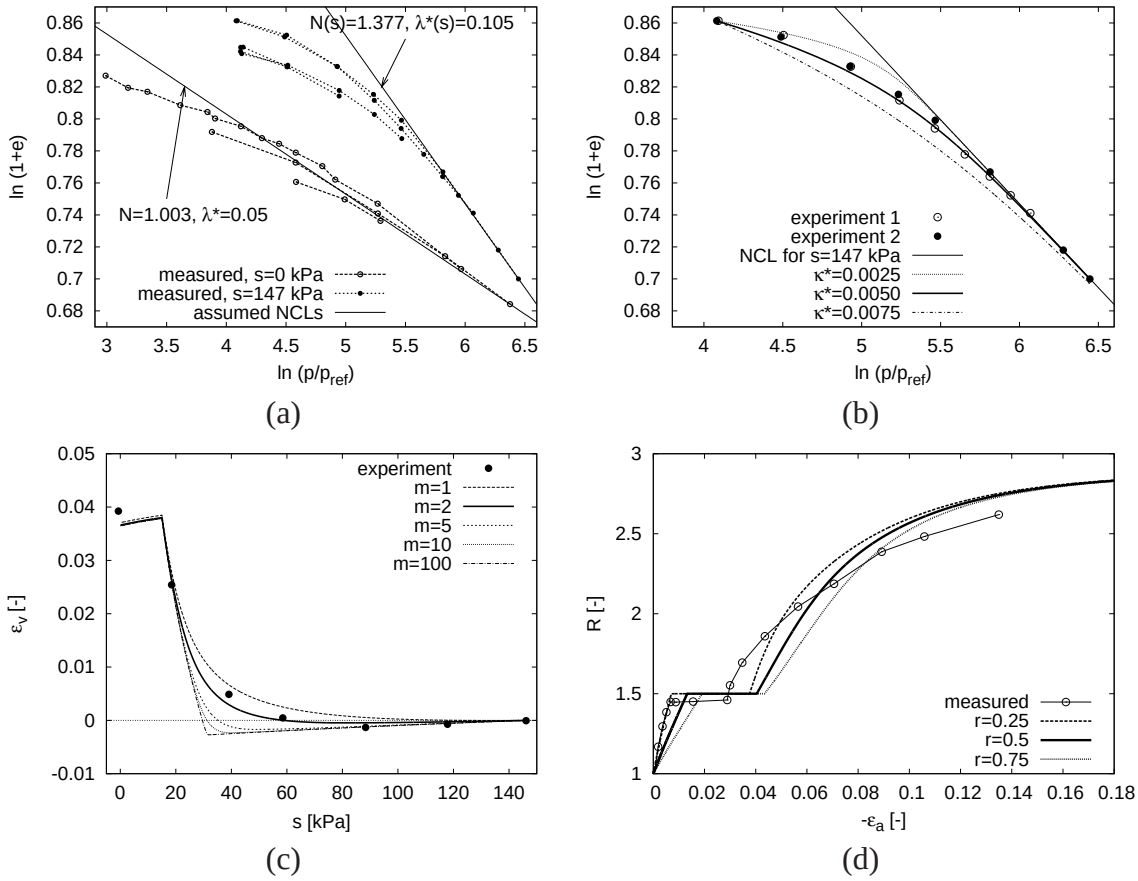

Figure 4: Calibration of the proposed model by means of experimental data on Pearl clay by Sun et al. [45]. (a) calibration of parameters N, λ^*, n and l by means of isotropic compression test with constant suction ($s = 0$ kPa and $s = 147$ kPa); (b) calibration of κ^* using isotropic compression test at $s = 147$ kPa; (c) calibration of m using constant net stress wetting test; (d) calibration of r using constant net mean stress shear test at constant suction $s = 0$ kPa and $s = 147$ kPa (with wetting at $R = T_a/T_r = 1.5$).

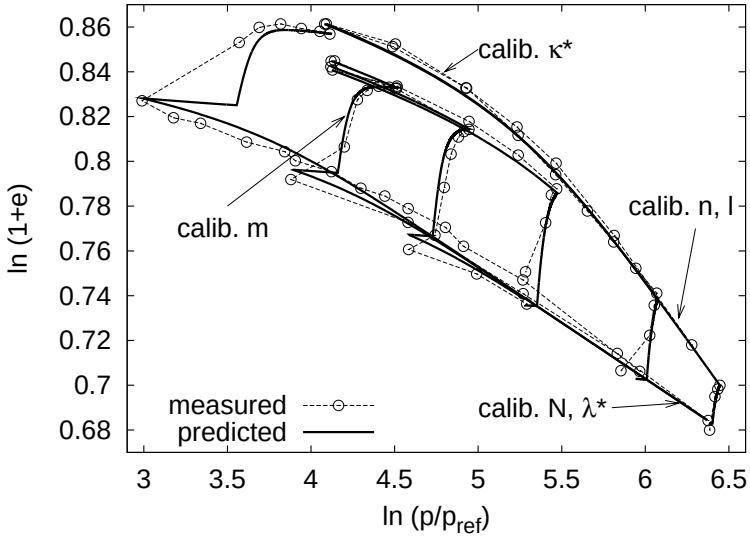

Figure 5: Isotropic compression tests at constant suction and wetting tests at constant net stress by Sun et al. [46] replotted in the effective stress space with superimposed predictions by the proposed model. Tests used for calibration of model parameters are indicated.

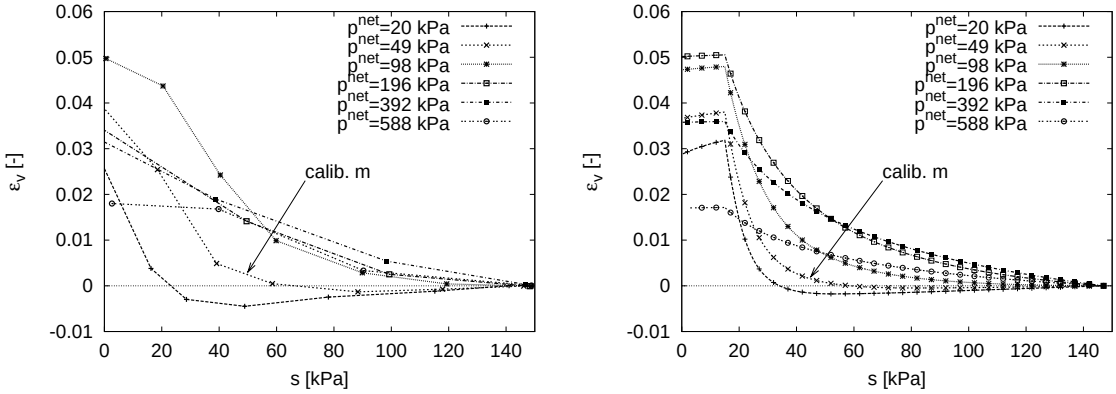

Figure 6: Wetting tests at constant isotropic net stress by Sun et al. [46] plotted in s vs. ϵ_v plane (a) and predictions by the proposed model (b). Test used for calibration of parameter m is indicated.

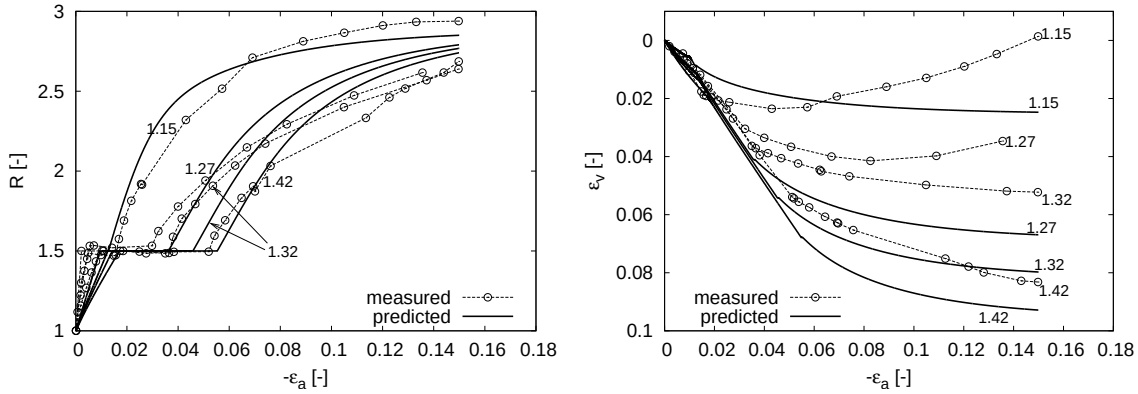

(a) (a)

Figure 7: Constant net mean stress shear tests and constant $R = 1.5$ wetting tests on specimens with different initial void ratios, experimental data by Sun et al. [46] and predictions by the proposed model plotted in ϵ_a vs. $R = T_a/T_r$ plane (a) and ϵ_a vs. ϵ_v plane (b). Labels for initial void ratios.

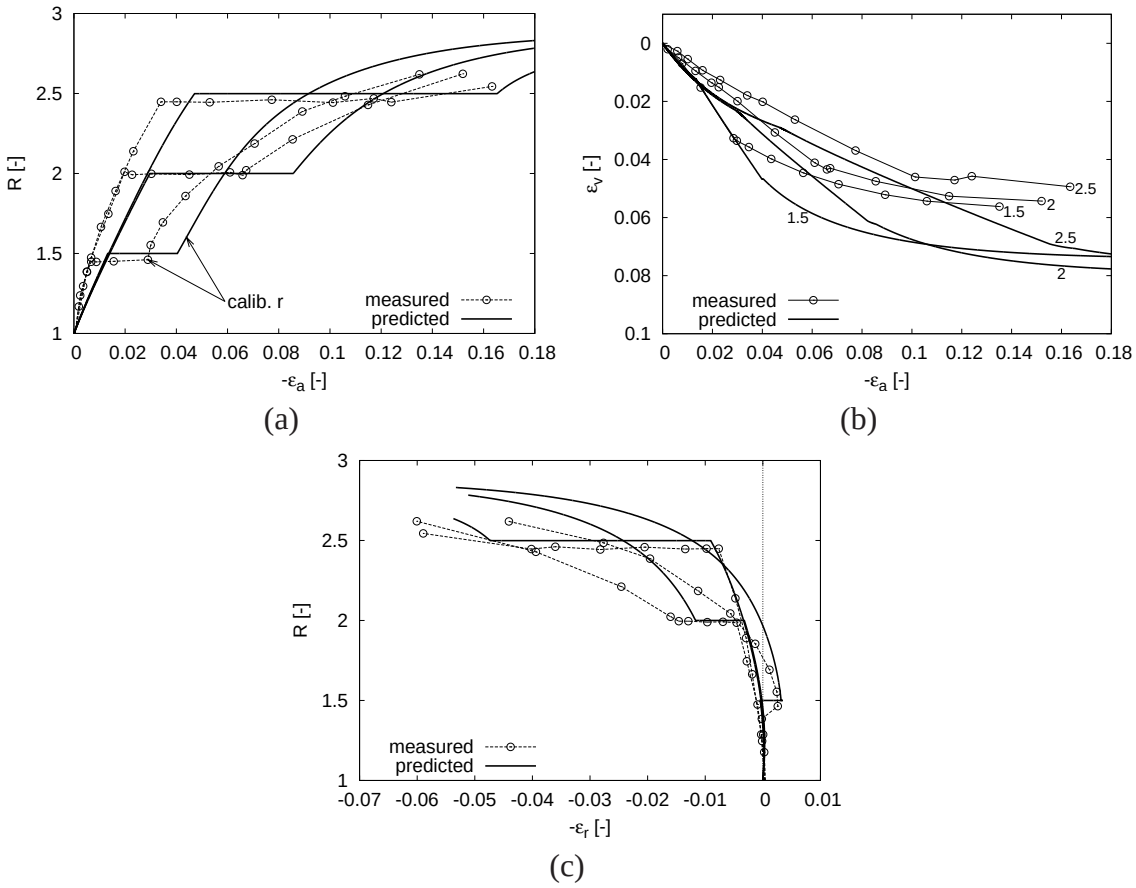

Figure 8: Constant net mean stress compression shear tests and constant R wetting tests, experimental data by Sun et al. [46] and predictions by the proposed model plotted in ϵ_a vs. $R = T_a/T_r$ plane (a) ϵ_a vs. ϵ_v plane with labels for R at wetting (b) and ϵ_r vs. $R = T_a/T_r$ plane (c). Test used for calibration of parameter r is indicated. Initial values of e: R at wetteing equal to 1.5, $e_0 = 1.29$; $R = 2$, $e_0 = 1.31$; $R = 2.5$, $e_0 = 1.3$.

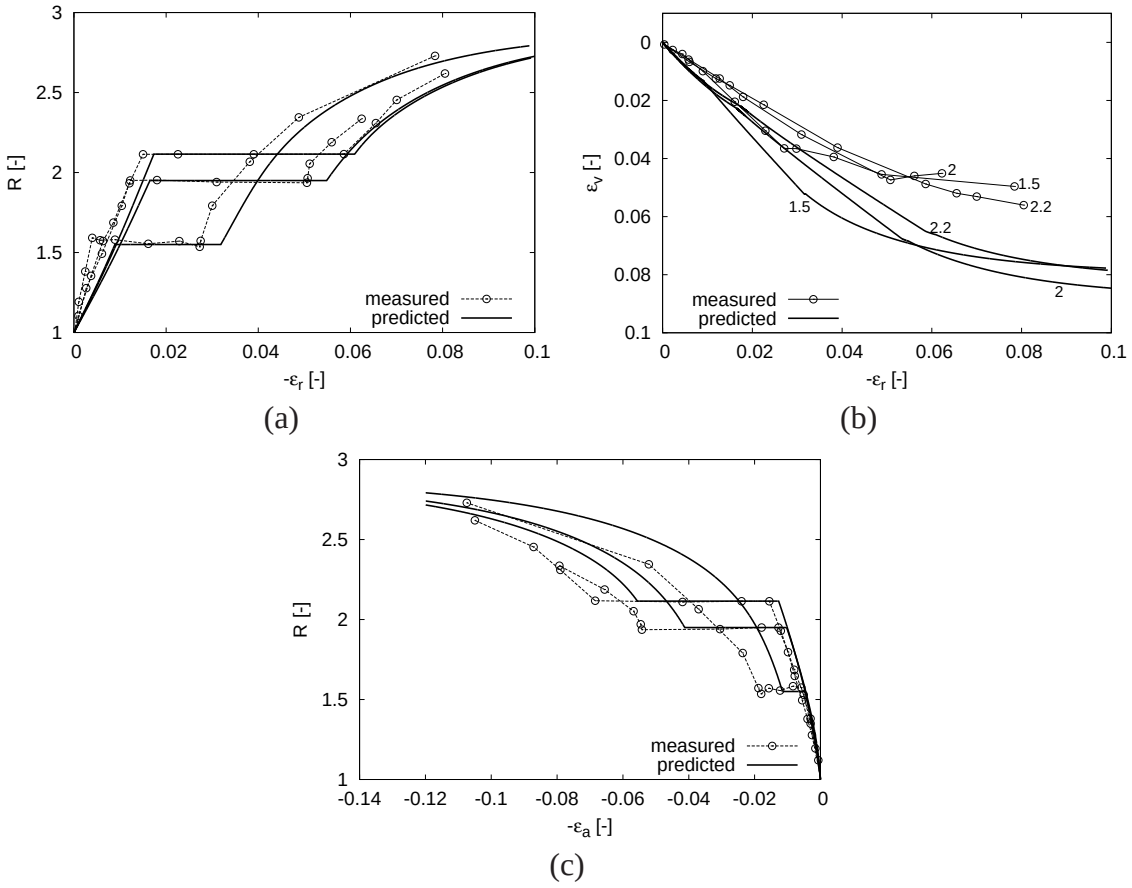

Figure 9: Constant net mean stress extension shear tests and constant R wetting tests, experimental data by Sun et al. [46] and predictions by the proposed model plotted in ϵ_r vs. $R = T_r/T_a$ plane (a) ϵ_r vs. ϵ_v plane with labels for R at wetting (b) and ϵ_a vs. $R = T_r/T_a$ plane (c). Initial values of e: R at wetteing equal to 1.5, $e_0 = 1.31$; $R = 2$, $e_0 = 1.35$; $R = 2.2$, $e_0 = 1.32$.

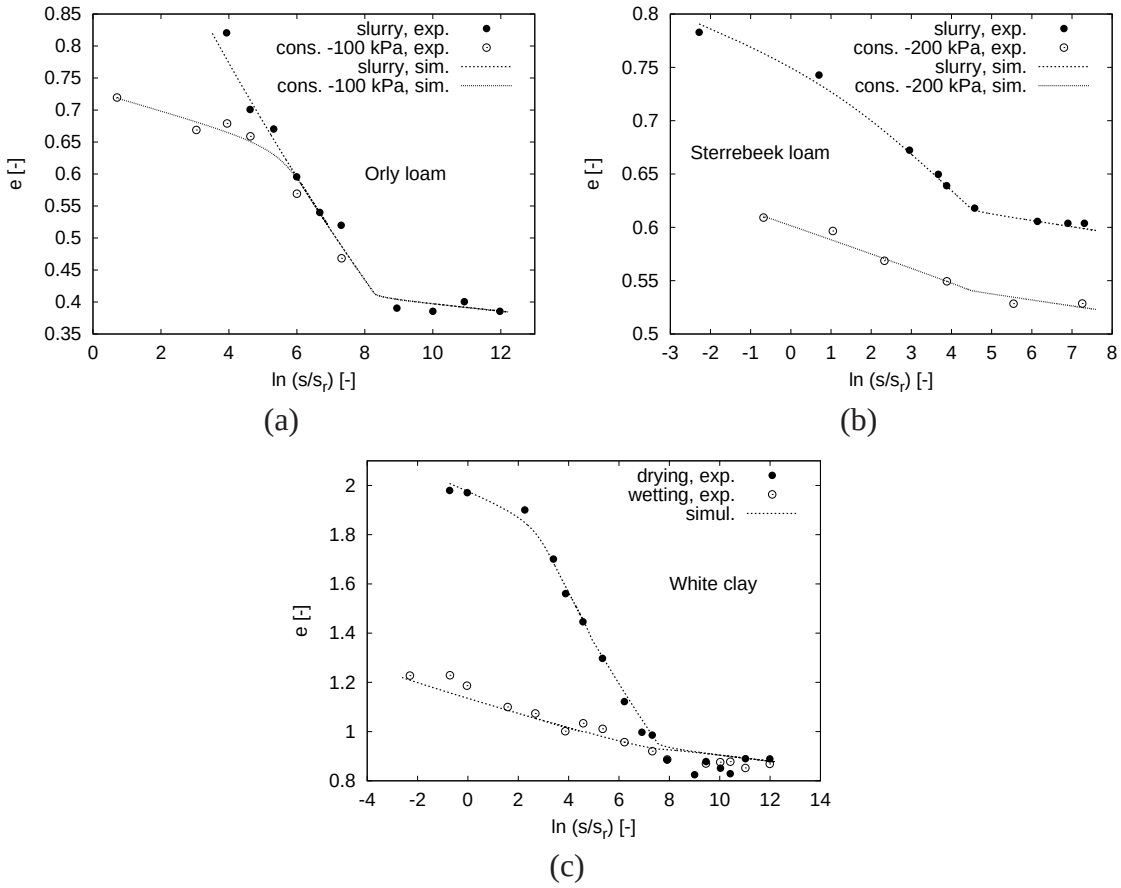

Figure 10: Drying (a, b) and drying-wetting (c) tests on different soils. Experimental data by Fleureau et al. [12] compared with simulations by the proposed hypoplastic model. s_r is a reference value of suction equal to 1 kPa.

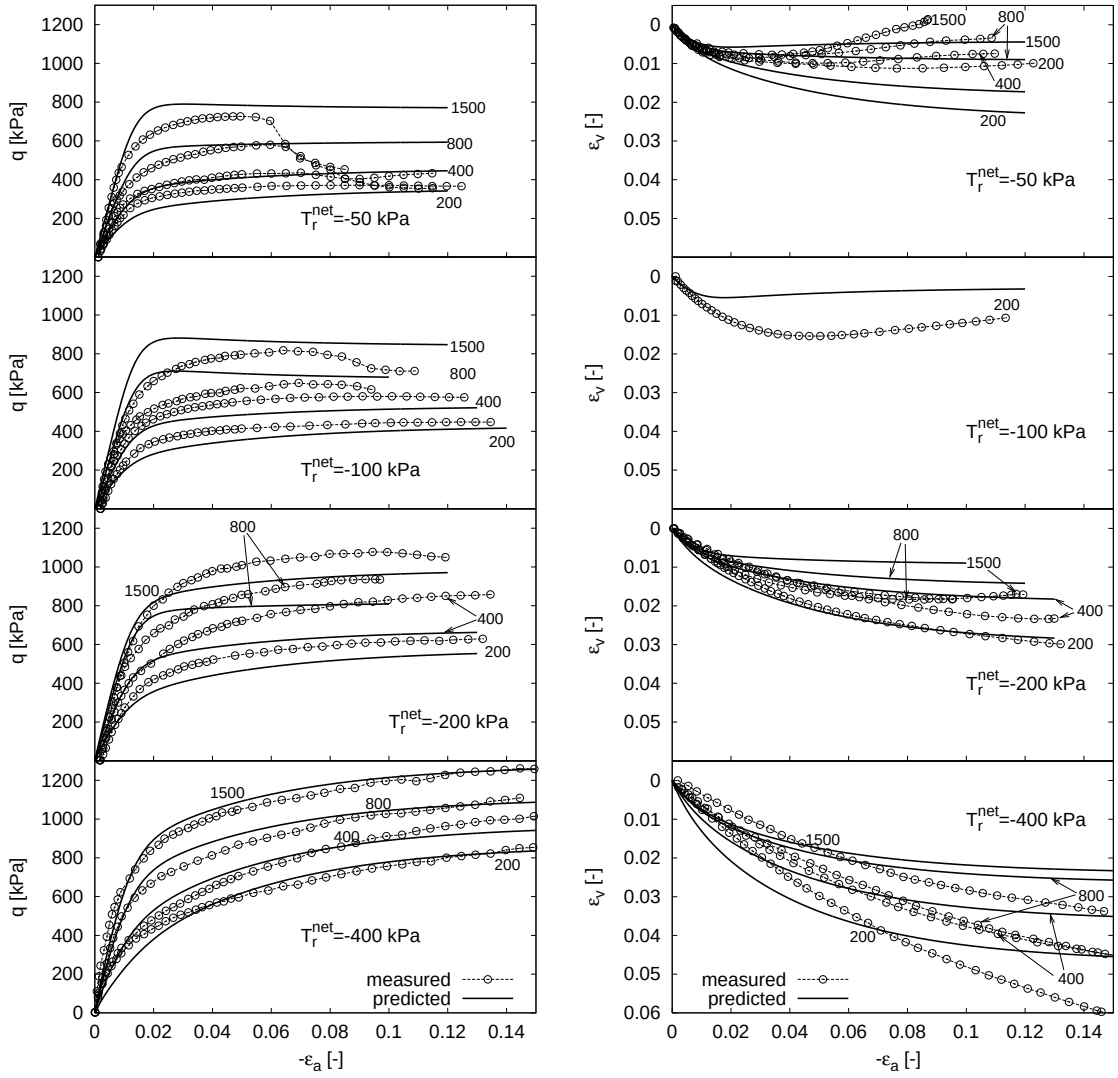

Figure 11: Drained triaxial tests on Jossigny loam at different suctions and net cell pressure levels, experimental data from Cui and Delage [9] and simulations by the proposed model. Deviatoric stress ($q = -(T_a - T_r)$) vs. axial strain curves (a) and volumetric vs. axial strain curves (b) with labels for s (in kPa).